# Fast Tuning And Comparison Of Predictive Functional Control Strategies

**Jean-Yves Dieulot, Frédéric Colas, Tarik Benhammi, Pierre-Jean Barre, Pierre Borne**

*CEMODYNE / L2EP, ENSAM, 8 Bd Louis XIV, 59000 Lille, France*
*LAGIS/ Ecole Centrale de Lille, BP 48, 59651 Villeneuve d'Ascq, France*

***Abstract:*** *Different predictive control strategies have been validated on a high-speed flexible manipulator. It has been shown that the use of a rigid model instead of a flexible two-mass-spring model could enhance the tuning procedure of Predictive Functional Control, and that the use of adequate trajectory planning is essential to ensure the cancellation of vibrations. Cascaded predictive control, which consists of a cascaded loop where the traditional servo algorithms are replaced by PFCs, could minimize the peak vibrations and dramatically enhance the cycle time. Predictive Functional Control alone is simpler to tune and can exhibit comparable performances, except that the controller is more sensitive to nonlinear phenomena such as dry friction, which were not taken into account into the model and generate a static error.*

***Keywords:*** *Model-based control, Robot control, Predictive control, Trajectory Planning.*

## 1. INTRODUCTION

Modern high-speed Cartesian robots are widely used for handling purposes, for example in automotive and plastic industries. Linear axes devoted to pick-and-place applications undergo high accelerations and speeds, which, combined with the economic demand for lighter structures, generates undesirable vibrations at the manipulator end-effector.

The traditional cascaded-loop servo algorithm consists of a current, a speed and a position loop, for which the individual controllers within each loop use Proportional or PI algorithms [1,2], and are thus easy to tune. This control strategy is unable to handle flexible structures, for which the tracking lag that cumulates through the loops makes it impossible to cancel properly the oscillating poles and zeroes [3,4].

There is thus a need for advanced control algorithms handling flexible structures, and, among those, this paper investigates the use of the Predictive Functional Control Algorithm which embeds both feedforward and a servo algorithms and which is known for its tracking abilities – due to multiple-step-ahead prediction – and robustness with respect to model uncertainties [5-9].

Whereas Predictive Functional Control was often applied to the control of rigid bodies [10], it has also been used to drive flexible axes (e.g. [11]), but tuning the control parameters is a difficult task. When there exists high uncertainties on the damping ratio or the natural frequencies, PFC derived from a flexible model does not yield good results. A so-called decomposition principle has been introduced which splits up the model into the sum of a fictitious model with better damped poles and another model which accounts for flexible modes and will be seen as a disturbance of the first model [12]. However, the main drawbacks of this method are the need for a preliminary black-box model identification and the arbitrary design of the fictitious model, which do not allow to account for the physical characteristics of the manipulator. Since predictive control is not easily applicable to flexible structures it is possible to use a cascaded control strategy where both position and speed loops can be replaced by a predictive controller with better tracking abilities [13,14].

However, these cascaded predictive algorithms have not been applied previously to flexible structures. Moreover, the overall tuning procedure used for prediction and control design has to be simplified in order to avoid the aforementioned problems.

In addition to the servo controller, the basic control structure of a linear axis includes a trajectory planning and a feedforward term (Fig. 1). Most Predictive Servo Controllers are used along with a time-optimal trajectory planning motion (under speed and acceleration constraints, called a *bang-bang in acceleration*), which involves discontinuities in acceleration, thus generating end-effector vibrations. However, a properly tuned bang-bang profile in jerk – the derivative of acceleration – is able to cancel perfectly vibrations [15, 16] while being near time-optimal and robust with respect to model uncertainties [17].

A first novelty of this paper consists of combining the tracking performances of the PFC controllers with appropriate trajectory planning. Next, since there is a need for easy tuning of PFC controllers when applied to flexible structures, a cascaded-loop strategy will be proposed. The controller will be designed using a global rigid model for which parameters are easy to obtain from the physical characteristics of the manipulator.

The organization of the paper is as follows: first, the basic model of a flexible structure and trajectory planning methods will be recalled. PFC controller will be presented, and several control strategies (industrial loop, cascaded PFC, composite cascaded PFC) will be proposed. An experimental comparison will be drawn for the control of a highly flexible pick-and-place robot, which will allow to quantify the contributions of the PFC cascaded controllers.

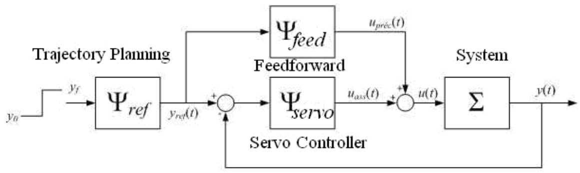


Fig. 1. Control Structure of a linear axis

## 2. GENERIC MODELLING OF A FLEXIBLE STRUCTURE

Many different and complementary strategies can be considered when trying to identify vibration modes and deriving a model for control, because continuous flexible systems exhibit an infinite number of modes. In this paper, only the dominant mode (with the lowest frequency) will be considered, because, in the practical application, the other modal frequencies are rather high. The modes and modal parameters (frequency, damping) can be obtained by experimental modal analysis [18], Finite-Element Modelling (FEM) [19] or with a beam-assembly model using Assumed Mode Methods [20,21]. Whereas black-box models can be used as a basis for local modelling and control around a set-point, their parameters cannot be related to the mechanical properties of the structure. Moreover, to be effective, this long preliminary procedure should be repeated for many local points and every machine, which is impossible in practice. Single-mode models such as two-mass spring models are widely employed to approximate the dynamic behavior of mechanical systems, [3, 4], and their relation to the physical parameters depend mostly on the modelling method. In Fig. 2, basically, $m_1$ accounts for the motor modal mass, $m_2$ accounts for the mass of the load, the transfer functions are given below (see [3] for full details and relations linking the resonant frequencies to the stiffness $k$ and viscous damping $c$).

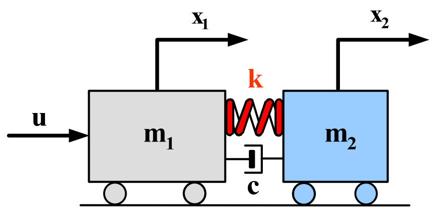


Fig. 2. 2-Mass-Spring Damper

$$H_1(s)=\frac{x_1(s)}{u(s)}=\frac{1+\frac{2\varsigma'}{\omega_n'}s+\frac{1}{(\omega_n')^2}s^2}{m_{tot}s^2\left(1+\frac{2\varsigma}{\omega_n}s+\frac{1}{\omega_n^2}s^2\right)},$$

$$H_2(s)=\frac{x_2(s)}{x_1(s)}=\frac{1}{1+\frac{2\varsigma}{\omega_n}s+\frac{1}{\omega_n^2}s^2} \tag{1}$$

where $m_{tot}=m_1+m_2$, $r=\frac{\omega_n'}{\omega_n}$ is the inertia ratio, $\zeta_n',\zeta_n$ are the damping ratios of the numerator and denominator of $H_1(s)$, $\omega_n,\omega_n'$ are the resonance and anti-resonance frequencies. The transfer function $H(s)=\frac{1}{m_{tot}s^2+f_v s}$ (2) corresponds to the rigid mode, where $f_v$ is an additional viscous friction coefficient. This rigid model is very easy to obtain from a single experiment [4].

Note that, in practice, $m_2$ is controlled only in open-loop because of the lack of sensors on the end-effector, which often arises in 3D-manipulators, for costs reasons. In the paper, the measurement of the load position is only used for validation and not in the control algorithms.

## 3. INDUSTRIAL CONTROL AND ADEQUATE TRAJECTORY PLANNING

The industrial cascaded-loop controller consists of a current loop which has a high dynamics and is thus neglected, a speed loop which involves a PI structure and a position loop with only a proportional controller [1]. The speed controller is simply $C(s)=k_v\left(1+\frac{1}{\tau_v s}\right)$ where $k_v$, $\tau_v$ are the speed loop proportional gain and integral time constant. This controller is unable to drive perfectly the motor mass $m_1$ in the mass-spring model of Fig. 2 for which the transfer function involves both undamped zeros and undamped poles [3, 4].

When industrial 3-D Cartesian manipulators are considered, only the motor is controlled in closed-loop. Due to the resonance, even when the mass $m_1$ is perfectly controlled, the end effector position (mass $m_2$), which is controlled in open-loop, oscillates when the trajectory involves discontinuities in acceleration. As an alternative to minimum-time profile with constraints in speed and acceleration (known as a bang-bang in acceleration), a bang-bang profile in jerk (the jerk is the derivative of the acceleration) is proposed, for which the vibrations created by a positive pulse in jerk are cancelled when those generated by the converse negative pulse are in phase opposition, i.e. when [16],

$$T_j=\frac{2\pi}{\omega_n}, \tag{3}$$

where $\omega_n$ is the resonant frequency, $T_j$ is the duration of the jerk pulse (Fig 3). A discrepancy in 20 % in the modal frequency only generates 6 % (with respect to bang-bang in acceleration) peak oscillation. However, the overall vibration compensation is effective only with a good tracking of the motor position $x_1$, which requires the introduction of more complex servo control structures, such as Predictive

Functional Control. However, PFC is always used with a simple bang-bang profile in acceleration, which motivates the combination of both predictive control and vibration damping motion planning profiles.

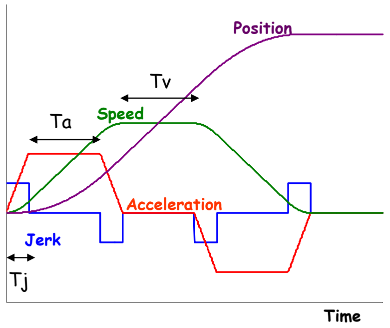


Fig. 3. Jerk Profile. $T_j$, $T_a$, $T_v$ are the constant jerk, acceleration and speed durations

## 4. PREDICTIVE FUNCTIONAL CONTROL

### *4.1 Basic concept*

In this section, the outline of model PFC algorithm, which is fully detailed in [6, 7] is recalled. PFC is based on a discrete linear model,

$$\begin{cases} x_M(n+1) = F_M x_M(n) + G_M u(n) \\ y_M(n) = C_M^T x_M(n) \end{cases} \tag{4}$$

$x_M$ is the state variable, $u(n)$ is the input, $y_M$ the system output, $F_M$, $G_M$, $C_M$ are constant matrices, $n$ is the sample number.

The predictive control strategy is summed up in Fig. 4. A control sequence is designed to enforce the model output to stick to a reference trajectory $y_R$ at given coincidence points. Over this receding horizon, the reference trajectory which is the path to the future set point, is resetted at every instant and is given by:

$$C(n+i) - y_R(n+i) = \alpha^i.(C(n) - y_P(n)), 0 \le i \le h, \tag{5}$$

$C(n)$ is the set-point, $y_P(n)$ the real process output, $\alpha : 0 \le \alpha \le 1$ is a parameter which represents the exponential convergence of the algorithm, and thus fixes the closed-loop behavior, $h$ is the prediction horizon.

### *4.2. Computation of control*

The future controls sequence should optimize the performance index (6) which turns to find the minimum in the least-square sense of the tracking error at fixed set-points – coincidence points– with respect to the future control sequence:

$$D(n) = \sum_{j=1}^{n_h} \{\hat{y}_P(n+h_j) - y_R(n+h_j)\}^2. \tag{6}$$

where $n_h$ is the number of coincidence time points $h_j$, $\hat{y}_P$ is the predicted output.

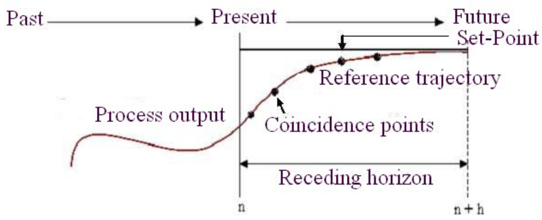


Fig. 4. Principle of PFC control

In order to compute easily the control algorithm, it will be assumed that the controlller is a composition of a priori orthonormal base functions (usually time-dependent polynomials $U_{B_k}(i) = i^{k-1}$),

$$u(n+i) = \sum_{k=1}^{n_B} \mu_k(n).U_{B_k}(i), i \ge 0, \tag{7}$$

where $\{U_{B_k}\}, k = 1 \cdots n_B$ are the $n_B$ base functions, the optimization problem reducing to find the corresponding weights $\{\mu_k\}_{k=1,n_B}$.

Of course, one could apply the whole control sequence, but, in fact, only the current control (8) is used, and the whole algorithm is computed again next step.

$$u(n) = \sum_{k=1}^{n_B} \mu_k(n).U_{B_k}(0) \tag{8}$$

For computational purposes, the model output is divided into a free (unforced) response, where the control is set to zero, and a forced response to the control (7).

$$y_M(n+i) = y_F(n+i) + y_{UF}(n+i), 1 \le i \le h, \tag{9}$$

where $y_F(n+i) = \sum_{k=1}^{n_B} \mu_k(n).y_{B_k}(i), 1 \le i \le h$ is the forced output, and $y_{B_k}$ is the response to the base function $u_{B_k}$, $y_{UF}(n+i) = C_M^T (F_M)^i x_M(n)$ is the unforced output.

Let the predicted future error be approximated by a polynomial function:

$$\hat{e}(n+i) = e(n) + \sum_{i=1}^{d_e} e_m(n) i^m, \tag{10}$$

where $d_e$ is a fixed approximation degree, and $e_m$ are coefficients. In the same way, the reference trajectory $c(n+i)$ can be decomposed in a polynomial with coefficients $c_m$.

Finally, the controller is obtained by setting $\frac{\partial D(n)}{\partial \mu_k} = 0$ (see [7], for details). Since the model output depends on the control, and hence on the $\mu_k$, these can be found from a Least-Square method, and the control parameters will only depend on the base functions, the convergence exponent and the coincidence points and can be computed off-line:

$$u(n) = k_0\{c(n) - y_p(n)\} + \sum_{m=1}^{\max(d_c,d_e)} k_m\{c_m(n) - e_m(n)\} + v_x^T x_M(n) \quad , \tag{12}$$

where, $d_c$ is the degree of the polynomial approximation of the set-point, and

$$k_0 = v^T \begin{bmatrix} 1-\alpha^{h_1} \\ 1-\alpha^{h_2} \\ \vdots \\ 1-\alpha^{h_{n_h}} \end{bmatrix}, \; k_m = v^T \begin{bmatrix} h_1^m \\ h_2^m \\ \vdots \\ h_{n_h}^m \end{bmatrix}, \; v_x = \begin{bmatrix} C_M^T(F_M^{h_1} - I) \\ C_M^T(F_M^{h_2} - I) \\ \\ C_M^T(F_M^{h_{n_h}} - I) \end{bmatrix}^T v$$

$$v = \left( \sum_{j=1}^{n_h} y_B(hj) y_B(hj)^T \right)^{-1} \left[ y_B(h_1) \dots \; y_B(h_{n_h}) \right] U_B(0)$$

The algorithm consists thus of a feedforward term devoted for tracking error, a disturbance rejection term and of a state-space controller $v_x^T x_M(n)$ .

Of course, since the problem is unconstrained, the predictive controller will be linear (else, see [22]); such a controller could be found by LQG or $H_\infty$ methods. Previous works [3] have shown that LQG could provide good results but was quite difficult to tune with a non-systematic design procedure (trial and error search of weight matrices) and that $H_\infty$ methods yield higher order controllers – which are not easily adapted in a generic way to the structure considered. In the application considered, control tuning will involve a "flat " prediction $\left(\hat{e}(n+i) = e(n)\right)$ and a convergence rate $\alpha$ , the parameters will be chosen with a rule of thumb [7] as

$$\alpha = e^{\frac{-3Te}{CLRT}} , \tag{13}$$

along with three coincidence points $H = \{h_i\}$ ,

$$H = (\left[\; CLRT/3 \quad CLRT/2 \quad CLRT \right] / T_e) , \tag{14}$$

where CLRT is the closed-loop rise time and $T_e$ is the sampling period. Note that the weighted sum of square errors at the coincidence points given in (14) should be minimum.

### *4.3 Predictive Functional Control strategies*

One of the main contributions of this paper consists of a fast tuning of the PFC algorithms, using simply a generic rigid model instead of the flexible model in Fig. 2 and of the "decomposition principle" (see e.g.[12]). In practice, the amplitude of the black-box model output is highly dependent on the damping factor when sufficiently small, and, thus, the prediction given by the flexible model is not good. Simulation results (not displayed in this paper) show that PFC obtained from a flexible model with 100 % variation on the damping ratio and 20 % variation on the modal masses exhibits poor results and can even lead to unstability. The philosophy of this paper follows, firstly by monitoring the center of gravity of the mass to be moved using a generic rigid model, letting the servo controller handle the flexible modes as a disturbance, and then by avoiding vibrations using an adequate trajectory planning.

As an alternative to the industrial cascaded controller or to a global controller (such as a PFC), a cascaded structure where the speed loop PI controller can be replaced by a speed loop PFC controller, hence realizing the decoupling of the inner and outer loop dynamics (see Fig. 5). When the position loop is a PI controller, the scheme will be called composite PFC controller, and when the position PI control is replaced by a PFC, the control scheme will be called a cascaded PFC. In the latter case, a PFC is embedded in the two loops.

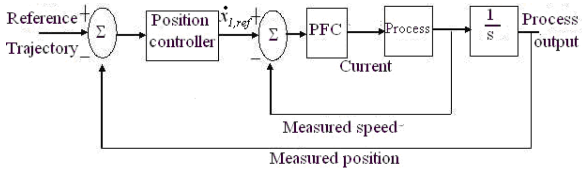


Fig. 5. Composite or Cascaded PFC controller

The rigid model (2) should thus be used for the design of the speed loop controller along with the specifications in (13-14), both for the composite controller and for the cascaded PFC.

However, when considering cascaded PFC, it will be assumed that the tracking of the reference trajectory of the speed loop is nearly perfect, i.e. that the speed closed-loop has a convergence rate of $\alpha$ as defined by equation (4). In this case, the position open-loop transfer function is

$$\frac{x_1}{x_{1,ref}} = \frac{1}{s\left(1 + s/\alpha\right)} , \tag{15}$$

and the speed loop reference is noted $\dot{x}_{1,ref}(t)$ (Fig. 5). The PFC in the position loop of the cascaded controller can be tuned using the transfer function (15).

To sum up, cascaded PFC control can be tuned with the help of a rigid model and assuming "perfect tracking" for the speed-loop. It will be shown in the experimental section that this strategy is effective when an appropriate motion planning is designed to damp vibrations.

## 5. CONTROL OF A FLEXIBLE ROBOT

The experimental validations are carried out on a 3-axes cartesian robot (Fig. 6) which has been equipped with a real-time "dSPACE 1103" control card. The geometry is quite simple since the cartesian axes can be considered as independent (axes coupling is negligible). Modal frequencies mostly depend on the position of the vertical and the orthogonal axis. When the horizontal axis is only moving, it will be considered that the axis stiffness remains almost constant and that the model is linear (the constant stiffness is $K = 1.27\ 10^5$ N.m ). The available measurements on the motor part come from the actuator axis encoders and is the only signal used for control. A laser sensor (measuring distance: 50 mm / measuring range: 20 mm) directly gives the load position, an accelerometer located on the end-effector gives the load acceleration and are only used for experimental verification.

The validation was undertaken for a displacement on the horizontal axis, with $y_2$ varying from $y_{2_0} = 0$ to $y_2 = 900$ mm, and the orthogonal axis position is set to 0 mm and the height of the vertical axis is set to 315 mm. An additional 12 Kg mass was carried to evaluate the robustness of the algorithms with respect to the mass of the load. This aspect is quite important, because the manipulator moves back-and-forth, picking and placing some piecework.

Fig. 6 Overview of the test-setup prototype (maximum feedrate: 120 m.min$^{-1}$, maximum acceleration: 4 m.s$^{-2}$).

For this specific control application, end-point precision is not mandatory, but the motor position should exhibit an overshoot less than 0.2 mm. The cycle time is set as the instant when the motor position is less than 0.5 mm from the set-point. The main requirement are thus in terms of motor and load peak vibrations and cycle time. The feedrate profile is a classical acceleration or jerk-limited bang-bang, i.e. the acceleration exhibits a square or a trapezoidal profile. Parameters of the industrial control loop -position and speed proportionnal gains - were $k_p = 14$ s$^{-1}$, $k_v = 2$ A.rd.s$^{-1}$.

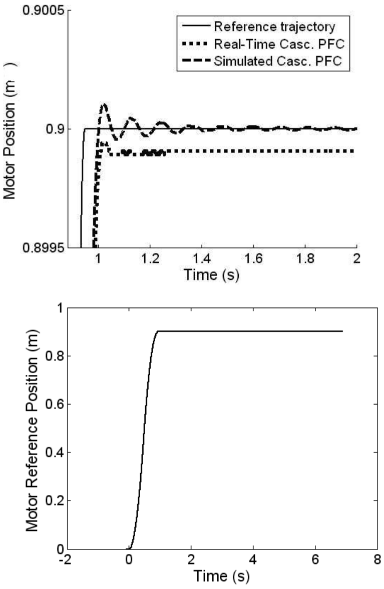


Fig. 7. Results of Simulations and Real-Time experiments

Fig. 7 shows that the simulations are in good agreement with the real-time experiments (note that the error is only by 0.05 mm). The cycle time is the same, and small discrepancies (oscillations and static error) are only due to the light dry friction phenomenon that was not taken into account into the model. Note that dry friction can be compensated by appropriate methods [23] but that the corresponding model parameters may vary with cycle repetitions and temperature rise. The PFC parameters were tuned from equations (13) and (14), using different trial and error simulations. The sampling period was set to $T_e = 0.5.10^{-3}\,s$. Best results were obtained for $CLRT = 100.T_e$ for PFC and both cascaded PFC loops and $CLRT = 150.T_e$. Note that cascaded PFC loop was not that easy to tune and that a too high $CLRT$ value in the position loop might lead to a degradation of the overall results.

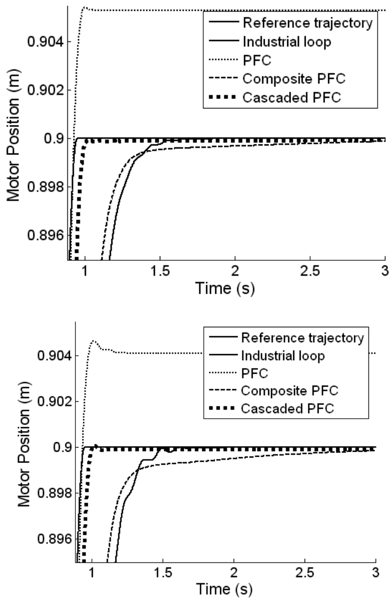


Fig. 8. Comparison of PFC algorithms/ motor control (with – up - and without –down - load)

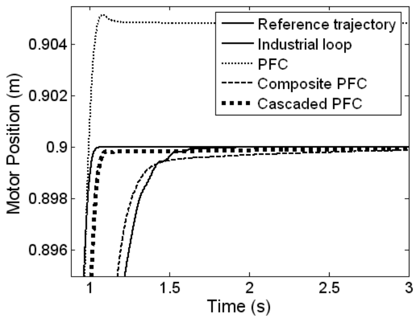


Fig. 9. Comparison of PFC algorithms/ motor control with jerk (no load)

A tracking lag is not acceptable because it will first increase the cycle time, and second, the position of the end-effector (mass $m_2$) is computed in open-loop from the motor position (mass $m_1$); an important tracking error will further result in bad end-efector behavior. In this respect, the industrial controller is unable to follow accurately the reference trajectory (there is an important –with respect to cycle time– tracking lag, which is not the case when using cascaded PFC) , and, when the gains are increased or when the load is changed, the position signal starts to oscillate. Composite PFC somewhat improves cycle time but the behavior is quite close that of the cascaded loop controller, except for oscillations; small discrepancies (dry friction…) in the model increase the time to reach the desired position (considering the above specifications, it does not increase the cycle time).

PFC, as a global controller which does not have to bear the lags introduced in the cascaded loops, is the fastest algorithm which is very interesting when the final precision is not important; however, as can be seen, the static error (even introducing an integrator into the controller) might be prohibitive. Cascaded PFC is the best algorithm from the performances point of view (cycle time and peak oscillation). However, one has to keep in mind the increasing complexity of the tuning (two PFC loops) with respect to other control structures.

Figures 8-9 show that all algorithms are robust with respect to an additional load or to a change in trajectory (bang-bang in jerk).

Fig. 10 shows the relevance of jerk control. With a perfect tracking and no jerk , mass $m_2$ behaves as a pure oscillator, which is the case for cascaded PFC, for which motor position tracking is very good but load oscillations are comparable to that of industrial control. When using a jerk trajectory, oscillations vanish for the cascaded PFC controller and the cycle time is greatly improved. Finally, the current shape is given in Fig. 11 for cascaded PFC control and industrial control: one can see that the oscillations coming from the flexibilities cannot be found in the drive current signal for PFC algorithms. However, the strategy of PFC which consists of calibrating the reference trajectory at each step causes small high frequency oscillations, which are not harmful for this manipulator, but should be filtered if necessary for flexible structures with significant auxiliary modes.

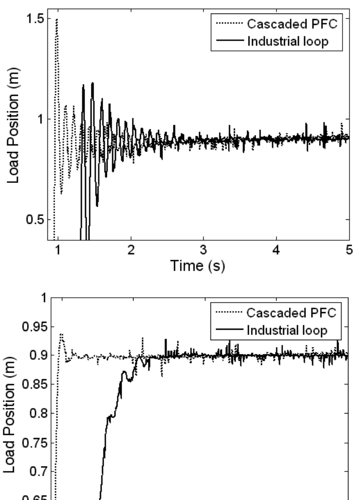


Fig. 10. Comparison of PFC algorithms with load (with and without jerk)

The more significant results are summarized in Tables 1 and 2 (see Appendix), and allow to evaluate the contribution of the cascaded PFC control strategies. Table 1 compares the cycle time for different control strategies to the conventional cascaded-PI controller where the position reference is a bang-bang in acceleration, with or without an additional load. PFC and cascaded PFC controls improve the cycle time by more than 30 % but PFC reduces the peak vibrations. Composite PFC does not yield good ersults, and it has been noticed experimentally that an increase of the position gain may lead to poor vibratory behavior. When PFC and cascaded PFC are used along ith a bang-bang in jerk trajectory (Table 2), the cycle time is improved by more than 25 %, and cascaded PFC allows to reduce the peak oscillation by more than 80 %, which shows the relevance of this control structure.

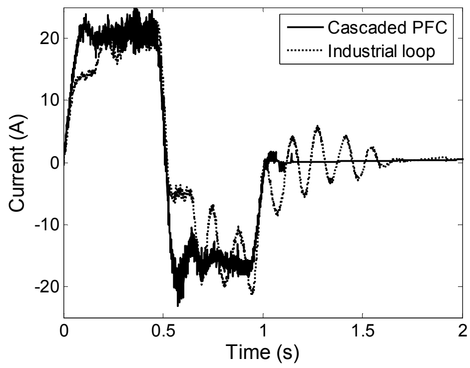


Fig. 12 Drive Current

## 6. CONCLUSION

Composite Predictive Functional Control algorithms – a cascaded structure where only the speed loop servo algorithms or both speed and position controllers were replaced by PFCs – were validated on a high-speed flexible pick-and-place robot. The tuning procedure was quite simple and involved the general rigid model which can be found from the physical characteristics of the robot and a single experiment (for the determination of the viscous friction parameter). The use of an adequate trajectory planning method, a bang-bang profile in jerk, was proven to be able to almost suppress the end-effector vibrations when the motor position was well tracked. Cascaded predictive control could minimize the peak vibrations by 90 % and enhance the cycle time (more than 30 % for the trajectory considered), with respect to industrial control). Classical PFC is easier to tune (only one PFC loop) , the closed-loop performances being nearly the same; however, the controller is more sensitive to unmodelled nonlinear phenomena such as dry friction, which were not taken into account into the model. The resulting static error can be unacceptable and alternative solutions have, in this case, to be proposed.

## 7. APPENDIX

**Table 1** Performances and Results of different controllers without jerk (reference is industrial control with bang-bang in acceleration). Un = Unloaded, Ld = with additional load, NO = no oscillations

| No Jerk | | | | | | |
|---|---|---|---|---|---|---|
| | PFC | | Casc. PFC | | Compos. PFC | |
| | Unl | Ld | Unl. | Ld | Unl. | Ld |
| Cycle Time (%) | **-34** | **-35** | **-30** | **-36** | +3 | +35 |
| Load peak oscill. (%) | **12** | 0 | -31 | **-10** | NO | NO |

**Table 2** Performances and Results of different controllers with bang-bang jerk profile (reference is industrial control with bang-bang in acceleration).

Un = Unloaded, Ld = with additional load, NO = no oscillations

| Jerk | | | | |
|---|---|---|---|---|
| | Ind Control | | PFC | |
| | Unl. | Ld | Unl. | Ld |
| Cycle Time (%) | + 2 | + 4 | **-32** | **- 31** |
| Load peak oscill.(%) | - 72 | - 75 | -73 | - 70 |
| | Casc. PFC | | Composite PFC | |
| | Unl. | Ld | Unl. | Ld |
| Cycle Time (%) | -26 | - 26 | + 8 | + 38 |
| Load peak oscill. (%) | **-91** | **- 83** | NO | NO |

REFERENCES


Armstrong-Helouvry, B., Dupont, P., & Canudas de Wit, C. "A survey of models, analysis tools and compensation methods for the control of machines with friction", *Automatica*, 30, **1083–1138,** 1994.

Barre, P.J., Béarée, R., Borne , P. & Dumetz, E., "Influence of a Jerk Controlled Movement Law on the Vibratory Behaviour of High-Dynamics Systems", *J. Intell. Robot. Systems*, 42, **275–293**, 2005.

Clarke, D. W., Mohtadi, C., & Tuffs, P. S. "Generalized predictive control. Part I: the basic algorithm. Part II: Extensions and interpretations." *Automatica*, 23, **137–160**, 1987.

Colas, F., Dieulot, J.-Y., & Barre P.-J. "A Quantitative Evaluation of the Non-Minimum Phase Phenomenon for a Robot Arm", *IMACS-IEEE-SMC Conference on Computational Engineering in Systems Applications*, Beijing, 2006.

Dieulot, J.-Y., Thimoumi, I., Colas, F., & Béarée, R. "Numerical aspects and performances of trajectory planning methods of flexible axes", *Int. J. Computers, Comm. and Control*, 4, **35–44**, 2006.

Dumetz, E.. Dieulot, J.-Y., Barre P.J., Colas, F., & Delplace, T. "Control of an industrial robot using acceleration feedback", *J. Intell. Robot. Systems*, 46, **111–128**, 2006.

Ellis, G. "Control system design guide" (2nd ed.), Academic Press, Boston, 2000.

Erkorkmaz, K., & Altintas, Y. "High-speed CNC system design. Part III: high speed tracking and contouring control of feed drives", *Int. J. Machine Tools & Manuf.,* 41, **1637 – 1658**, 2001.

Groß, H., Harmann, J., & Wiegârtner, G. "Electrical feed drives in automation", MCD corporate Publishing, SIEMENS, ISBN 3-89578-148-7, 2001.

Guemghar, K., Srinivasan, B., Mullhaupt, Ph., & Bonvin, D. "Analysis of cascade structure with predictive control and feedback linearization", *IEE Proceedings-Control Theory and Applications*, 152, **317 – 324**, 1995.

Harris, C.M. "Shock and Vibration Handbook" (fourth edition). New York: McGraw-Hill, 1996

Hedjar, R., Toumi, R., Boucher, P., & Dumur, D. "Two cascaded nonlinear predictive controls of induction motor", *Proc. IEEE Conf. Control Appl.,* 2003

J.-Y. Dieulot, F. Colas, "Robust PID control of a linear mechanical axis: A case study", *Mechatronics*, In Press, 2008.

Margolis, D.L. "Bond Graphs, normal modes and vehicle structures", Vehicle System Dynamics, 7, **49-63**, 1978.

Mayne D.Q., Rawlings J.B., Rao P.M.& Scokaert P.O., "Constrained model predictive control: stability and optimality", *Automatica*, 36, **789-814**, 2000.

Meirovitch L., "Fundamentals of Vibrations" (second printing). New York: McGraw-Hill, 2001

Richalet, J. "Industrial applications of model-based predictive control", *Automatica*, 29, **1251 – 1274**, 1993

Richalet, J., Abu, E., Arber C., Kuntze, H.B., Jacubasch, A.,& Schill, W.. "Predictive functional control. Application to fast and accurate robot". *10th IFAC World Congress, Munich, Germany,* 1997.

Richalet, J., Estival, J.L., & Fiani, P. "Industrial applications of predictive functional control to metallurgical industries", *Proc. 4th IEEE Conf. Control Appl.*, 934 – 942, 1995

Rossiter, J. A. "Predictive functional control: more than one way to prestabilise". *15th IFAC World Congress. Barcelona, Spain,* 2002.

Susanu, M., & Dumur, D. "Using Predictive Techniques within CNC Machine Tools Feed Drives", *44th IEEE Conf. Decision and Control*, 2005.

Vivas, A., & Poignet, P. 'Predictive functional control of a parallel robot', *Control Engineering Practice*, 13, **863 – 874**, 2005.

Yim W., & Singh S. "Nonlinear inverse and predictive end point trajectory control of flexible macro-micro manipulators", *J. Dyn. Dyst. Meas. Contr.*, 119, **412-420**, 1997.